

UniT: Unified Tactile Representation for Robot Learning

Zhengtong Xu, Raghava Uppuluri, Xinwei Zhang, Cael Fitch, Philip Glen Crandall, Wan Shou, Dongyi Wang, Yu She*

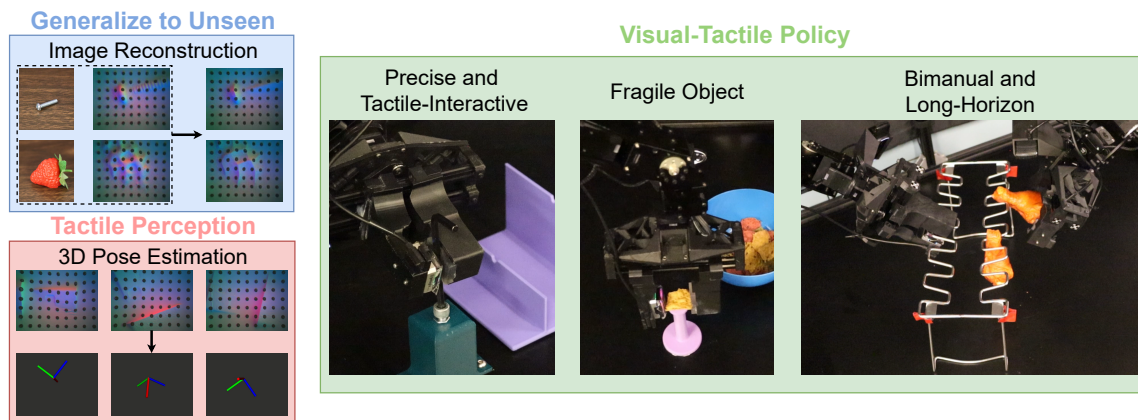


Fig. 1: UniT is a novel approach to learning a unified tactile representation with transferability and generalizability. This representation can be zero-shot transferred to various downstream tasks, including challenging perception tasks and policy learning for manipulation tasks involving rich robot-object-environment interactions.

Abstract—UniT is a novel approach to tactile representation learning, using VQVAE to learn a compact latent space and serve as the tactile representation. It uses tactile images obtained from a single simple object to train the representation with transferability and generalizability. This tactile representation can be zero-shot transferred to various downstream tasks, including perception tasks and manipulation policy learning. Our benchmarking on an in-hand 3D pose estimation task shows that UniT outperforms existing visual and tactile representation learning methods. Additionally, UniT’s effectiveness in policy learning is demonstrated across three real-world tasks involving diverse manipulated objects and complex robot-object-environment interactions. Through extensive experimentation, UniT is shown to be a simple-to-train, plug-and-play, yet widely effective method for tactile representation learning. For more details, please refer to our open-source repository¹ and the project website².

Index Terms—Representation learning, tactile sensing, imita-

*Address all correspondence to this author.

Zhengtong Xu, Xinwei Zhang, and Yu She are with the School of Industrial Engineering, Purdue University, West Lafayette, USA (E-mail: {xu1703, zhan4645, shey}@purdue.edu).

Raghava Uppuluri is with the Elmore Family School of Electrical Engineering, Purdue University, West Lafayette, USA (E-mail: ruppulur@purdue.edu).

Cael Fitch is with the School of Mechanical Engineering, Purdue University, West Lafayette, USA (E-mail: fitch2@purdue.edu).

Wan Shou is with the Department of Mechanical Engineering, University of Arkansas, Fayetteville, USA (E-mail: wshou@uark.edu).

Dongyi Wang is with the Department of Biological and Agricultural Engineering, University of Arkansas, Fayetteville, USA (E-mail: dongyiw@uark.edu).

Philip Glen Crandall is with the Department of Food Science, University of Arkansas, Fayetteville, USA (E-mail: crandall@uark.edu).

¹<https://github.com/ZhengtongXu/UniT>

²<https://zhengtongxu.github.io/unifiedtactile.github.io/>

tion learning.

I. INTRODUCTION

Imitation learning has shown promising results equipping robots in the domain of manipulation, with the ability to master complex, high-precision, dexterous skills through human demonstrations [1]–[4]. However, the predominant focus of current research is on leveraging image or point cloud inputs to perceive scene information. During manipulation, robots encounter varied force interactions from both the environments and the manipulated objects. The sole dependence on images [1]–[3] or point clouds [4], [5] could obscure critical details about the objects’ in-hand states and the dynamics of force interactions, which may be crucial for effective manipulation. Despite the current focus on visual information in robot learning research, humans routinely use visual and tactile feedback in manipulation tasks. Therefore, exploring the integration of visual and tactile modalities in imitation learning could potentially enhance the robots’ performance in manipulation tasks.

Vision-based tactile sensors such as GelSight [6] offer high-resolution feedback that captures extensive tactile information. In tactile sensing, GelSight has demonstrated the ability to perceive the geometry of the grasped object [7], the position and orientation of in-hand objects [8], [9], the normal and shear force fields [10], and even the physical properties of objects [11]–[13]. Moreover, recent studies incorporating vision-based tactile sensors into imitation learning have demonstrated their considerable potential

and improved performance [14]–[16]. Consequently, vision-based tactile sensors are highly effective for use in imitation learning for manipulation tasks.

Although incorporating visual-tactile feedback as policy input is a logical approach, it raises *Question 1*: Should we treat vision-based tactile feedback as typical visual input in robot learning? Treating it as such would imply that a system with tactile sensors is akin to one equipped with additional cameras, which could be processed by existing imitation learning frameworks.

However, does this approach truly capture the unique information of tactile feedback? Previous research indicates that the tactile images produced by GelSight, owing to their unique sensing principles, enable trained neural networks to exhibit strong generalizability. For example, a gradient estimation model trained solely on images from a small ball contacting the sensor can be generalized across objects with various shapes and textures [7], [17]. Similarly, a tactile-reactive grasping policy trained on standardized texture-less blocks shows generalizability to diverse objects with different shapes and textures [11]. Therefore, the generalizability demonstrated by GelSight highlights the distinctiveness of tactile images compared to standard visual images.

However, the tactile depth reconstruction and tactile reactive grasping models just discussed have only demonstrated generalizability within their respective specific tasks. Then, this leads to *Question 2*: Can we use a single simple object to learn a unified tactile representation that 1) possesses transferability and generalizability, and 2) incorporates as much of the rich information present in tactile images as possible? This representation would be advantageous in being applied in a zero-shot manner across a variety of downstream tasks involving different objects.

To address *Question 1* and *Question 2*, we propose UniT, unified tactile representation for robot learning, as shown in Fig. 1. Our contributions are summarized as follows:

1. Easy to Train yet Broadly Applicable: We introduce UniT, a tactile representation learning method for GelSight sensors. UniT uses VQVAE to learn a compact latent space and serve as the tactile representation. It can utilize data on a single simple object to learn a unified tactile representation that can be generalized to objects of different sizes and shapes. Through experiments in image reconstruction involving diverse objects, we demonstrate that the representation learned by UniT from a single simple object can capture information of unseen objects on contact configurations, object shapes, and dynamic marker motions induced by applied forces. This kind of transferability and generalizability makes UniT both straightforward to train and broadly applicable.

2. Deploy for Tactile Perception: The tactile encoder trained through UniT can be seamlessly transferred to downstream tactile perception tasks. Furthermore, due to UniT’s lenient data requirements during training, representations learned even from the simplest objects, such as a small ball, can effectively facilitate tactile perception of everyday objects. In experiments involving the task of estimating the in-hand 3D pose of the USB plug, UniT outperforms training

of a ResNet [18] from scratch, existing visual representation learning methods BYOL [19] and MAE [20], and the state-of-the-art tactile representation learning method, T3 [21].

3. Effective Visual-Tactile Policy Learning: In our framework, UniT can be integrated into visual-tactile imitation learning pipelines, achieving high-precision manipulation tasks with rich interactions. The experimental results show that for tasks involving substantial robot-object-environment interactions, policies incorporating UniT outperform those based solely on vision and those that treat tactile images as regular visual inputs.

II. RELATED WORK

A. Tactile-involved Imitation Learning

Existing tactile-involved imitation learning can be broadly categorized into three types: those utilizing low-dimensional tactile feedback, such as tactile arrays or force-torque feedback; those employing audio feedback; and those utilizing high-dimensional, vision-based tactile feedback.

Research that incorporates tactile arrays [22], [23], force-torque feedback [24], and in-hand audio feedback [25] into imitation learning policies have shown strong performance in tasks with complex interactions between environments, objects, and robots. However, tactile interactions are inherently complex and these modalities often do not capture the full spectrum of tactile information. For example, tactile arrays may struggle to accurately perceive an object’s geometry, in-hand position, and orientation, while force-torque and in-hand audio feedback may not effectively capture dynamic force distributions on the hand/finger.

Additionally, vision-based tactile sensors such as GelSight [6] offer high-resolution feedback that captures extensive tactile information. Recent studies incorporating GelSight into imitation learning have demonstrated its considerable potential and enhanced performance [14]–[16].

B. Representation Learning in Imitation Learning and Tactile Sensing

Recent studies demonstrate that representation learning significantly enhances performance in imitation learning [1], [26], [27]. Encoders that are pretrained with representation learning are particularly adept at extracting information from visual observations.

In the field of tactile sensing, a variety of representation learning frameworks have been introduced, including the use of MAE [28], [29] and CNN [30]. Furthermore, the work in [21] introduces a framework for tactile representation learning that scales across multi-sensors and multi-tasks. The work in [31] learns multimodal tactile representation by aligning tactile embeddings to pretrained image embeddings associated with a variety of other modalities.

In this paper, we demonstrate that using tactile images from single simple object can be used to train a tactile representation with transferability and generalizability. This ability to “train simply but work broadly” is not possessed by existing tactile representation learning frameworks.

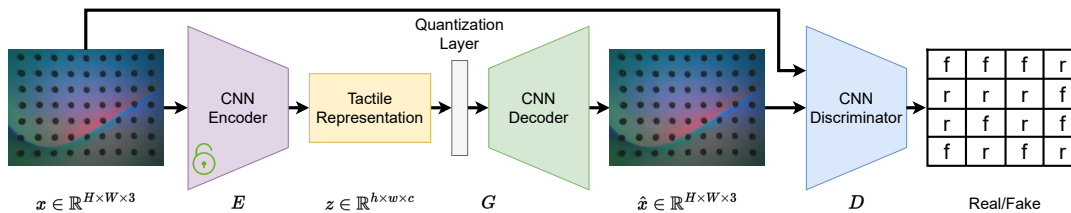


Fig. 2: Pipeline of UniT representation training.

III. METHOD

In this section, we detail our UniT pipeline and the integration of the pretrained encoders into downstream perception and policy learning tasks.

A. VQGAN Autoencoder

The work in [32] introduces VQGAN for high-resolution image synthesis. VQGAN integrates a vector quantized variational autoencoder (VQVAE) [33] with a patch-based discriminator. Subsequently, the work in [34] introduces latent diffusion model, which leverages the VQGAN autoencoder to compress images into a latent space where diffusion and denoising processes can occur. The efficacy of the latent diffusion model is largely due to the robust image compression capabilities of VQGAN, which not only facilitates high-quality image reconstruction but also avoids high degree of variance in the learned latent space through VQ regularization.

Although VQGAN demonstrates impressive performance in generative model and image generation areas, its role as an autoencoder is primarily to enable high-quality image compression and reconstruction. This function differs from the objectives of representation learning, which focus on capturing representations that distill the essential features of the original images (although reconstruction can be used to validate the effectiveness of representation learning). Such representations aim to generalize across a variety of downstream tasks, leveraging the unified features to perform diverse functions effectively. Therefore, for visual images, VQGAN may not necessarily be an ideal framework for representation learning.

Tactile images are derived from an imaging principle that combines RGB-tricolor light scattering with gel deformation. These images, produced by different objects, show different features. However, the color distribution of tactile images is significantly more compact than that of visual images. This compactness arises because tactile images are generated using the same imaging principles, which disregard the color of the object and background, focusing instead only on tactile features such as contact configuration, geometry, and force distribution. We believe that the compactness of tactile image distributions makes it possible to adequately represent these images in a more compact representation. Consequently, we utilize VQGAN for learning tactile representations.

As depicted in Fig. 2, the representation learning pipeline employs a VQGAN architecture with the quantization layer

absorbed into the decoder. This pipeline comprises a CNN encoder E , a CNN decoder (incorporating the quantization layer) G , and a patch-based discriminator D . The entire framework is trained in a self-supervised manner. Denote the tactile image input as $x \in \mathbb{R}^{H \times W \times 3}$, where the encoder E maps the image to a tactile representation $z = E(x) \in \mathbb{R}^{h \times w \times c}$. The decoder reconstructs z to an image \hat{x} .

The use of a discriminator is justified because recent studies [35], [36] have shown that adversarial loss can enhance the performance of representation learning. The presence of VQ regularization enables the learning of a compact tactile representation with reduced variance, which can improve the performance of representation learning based on the experimental results in Section IV.

B. Train with Simple and Single Object

In this section, training strategy is outlined as: training the autoencoder depicted in Fig. 2 using a single simple object to significantly simplify data collection. However, the UniT representation obtained through this training method exhibits transferability and generalizability.

In this paper, GelSight Mini with markers is used. We believe that other sensors from the ‘‘GelSight family’’ can also use our framework, as they share the same sensing principles. We chose the sensor pad with markers because it improves the tactile image’s capacity to capture the distribution of shear forces.

We present two training examples here: datasets were collected for two types of objects, an Allen key and a small ball, and autoencoders were trained for each, respectively. As depicted in Fig. 3, both the Allen key and the small ball have simple shapes and lack surface texture, suggesting that other similarly rigid objects could also be suitable for training. This leniency in selecting training objects demonstrates the simplicity and straightforwardness of our data acquisition and training processes.

The specific data collection process involves capturing images from the GelSight sensor at a fixed frequency (10 Hz), contacting the object with the GelSight, and continuously changing the contact configuration and the magnitude of the applied force.

The final size of our collected datasets includes 10,854 images of the Allen key and 4,831 images of the ball. Note that recording images at a frequency of 10 Hz enables the acquisition of such a dataset for a single object for no more than 20 minutes.

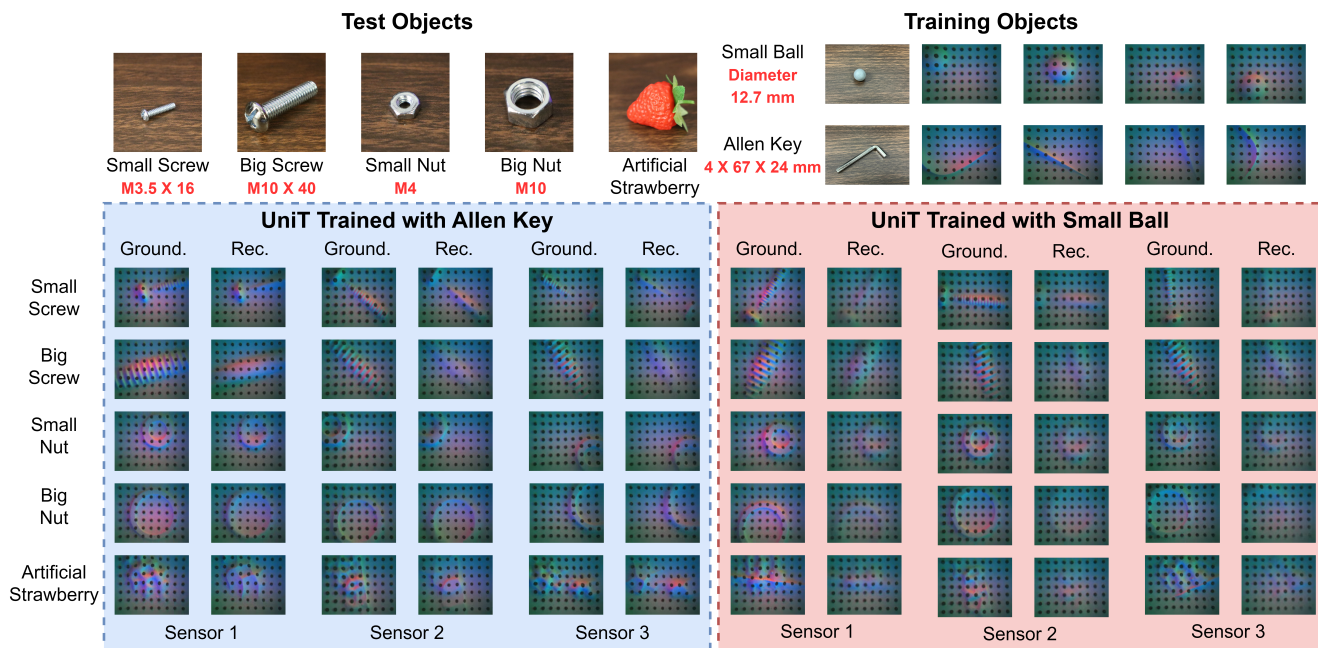


Fig. 3: Example results of UniT reconstruction of diverse unseen objects. Rec. represents reconstruction while Ground. represents groundtruth. Sensor 1, 2, and 3 are three different Gelsight Minis. One training dataset for the autoencoder is only collected on one sensor.

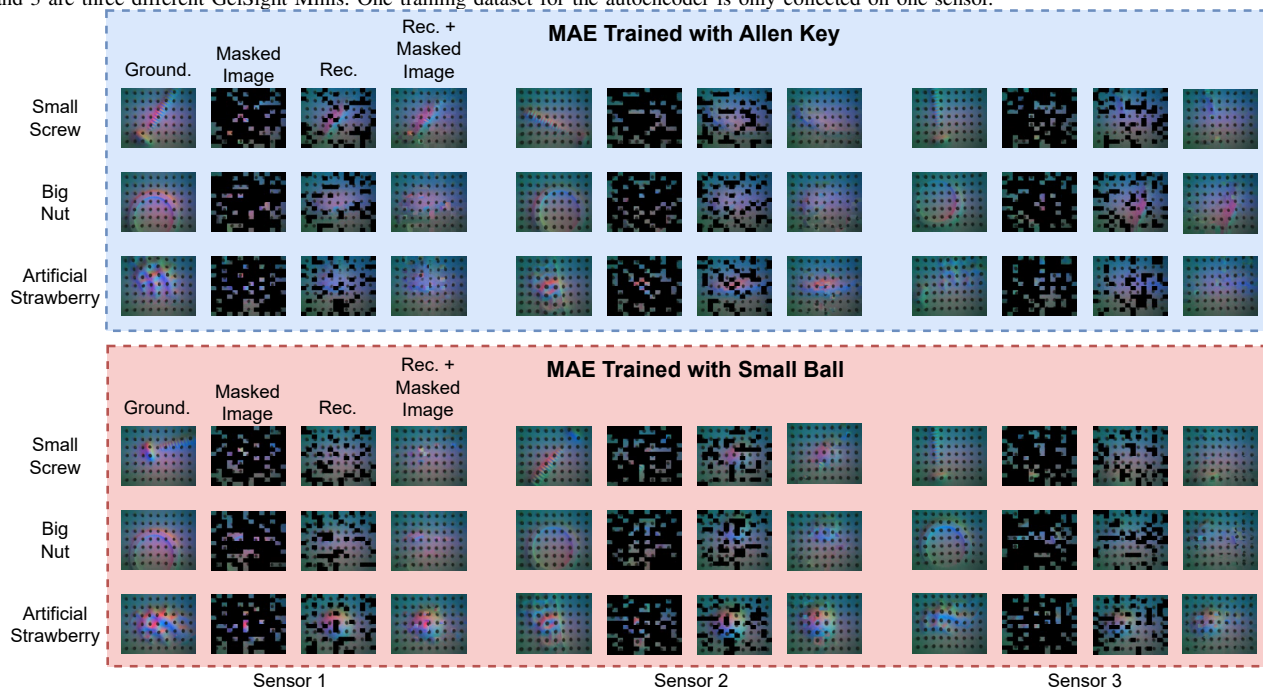


Fig. 4: Example results of MAE reconstruction of diverse unseen objects. We show the results of MAE with a ViT-Base backbone and a mask ratio 0.75 which is suggested by [20].

After completing the training for representation learning, experiments were conducted on image reconstruction using trained autoencoders across a series of unseen objects, as shown in Fig. 3. Moreover, comparing the performance of UniT with other methods, we conducted the same experiments using MAE [20], as illustrated in Fig. 4.

It is important to note that the reconstruction experiments conducted here are different from the depth reconstruction experiments shown in [7]. The goal of depth reconstruction is to generate depth images, whereas the purpose of image

reconstruction here is to verify whether the learned representation contains sufficient information from the original image. Therefore, the results of depth reconstruction and image reconstruction are not comparable, since they are not the same type of experiments.

Our experimental results indicate that although UniT was trained only on a single simple object, the learned tactile representation can effectively generalize to unseen objects with diverse shapes, sizes, and textures. This tactile representation can reconstruct images that preserve most of the critical

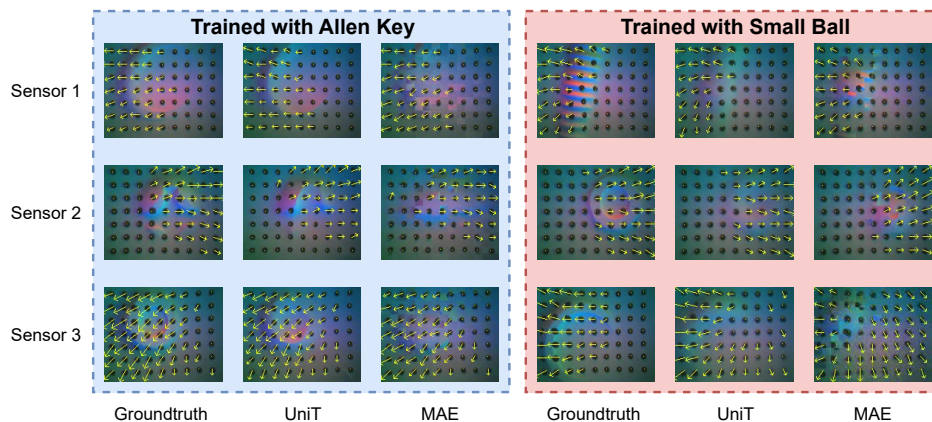


Fig. 5: Example results of marker tracking. To evaluate if the learned representations consist of information of the dynamic marker motion, we implement marker tracking [6] on groundtruth images and the corresponding image reconstructions by MAE and UniT.

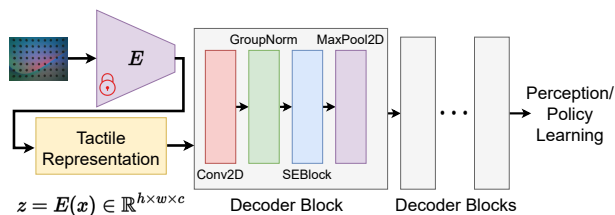


Fig. 6: Decoder architecture of implementing UniT representation to downstream tasks.

information of the original image, such as contact geometry and configuration (see Fig. 3). Moreover, the representation trained with an Allen key performs better than the one with the small ball. This is logical, as a small ball is one of the simplest objects from which to extract features: it lacks texture, edges, distinct shapes, and is omnidirectionally symmetrical. Despite this simplicity, the representation trained using a small ball can still capture features of unseen objects to a certain degree. Moreover, we have demonstrated that these representations can effectively generalize across different GelSight Minis, even though the training data originated from a single GelSight Mini.

Compared to UniT, MAE performs less ideal. In some cases, it can reconstruct the rough shape and orientation of the original object, but in other instances it fails to reconstruct. For example, as shown in Fig. 4, some artificial strawberry images are reconstructed as small ball images.

Finally, the marker tracking results are shown in Fig. 5, that demonstrate both UniT and MAE effectively capture the dynamic motion of markers. This capability is essential for applying these tactile representations in robot manipulation tasks with rich force interactions.

C. Decoder Head for Downstream Tasks

After completion of the autoencoder training, both the decoder and the discriminator are discarded. The encoder is subsequently connected to the proposed decoder blocks and then to downstream tasks (such as perception and policy learning tasks).

As shown in Fig. 6, for decoding the representation $z \in \mathbb{R}^{h \times w \times c}$, we utilize a decoder block consisting of Conv2D, GroupNorm [37], SEBlock [38], and MaxPool2D as the basic module. This arrangement is designed to extract the information contained in the representation z .

In the experiments given in this paper, we adopt a strategy where, after the representation learning phase is completed, the pretrained encoder is frozen when applied to downstream tasks, and only the decoder blocks are trained. Although it is certainly possible to fine-tune the UniT pretrained encoder for specific downstream tasks, the results in Sections IV and V demonstrate that this approach of freezing the encoder for zero-shot transfer already yields sufficiently good performance. This underscores the robust generalizability and transferability of UniT, which are important when applying tactile representations on various perception and policy learning tasks with different objects (see Section V), as fine-tuning for each task and each object can be prohibitively costly. Robust generalizability and transferability are crucial to utilizing the tactile modality to achieve highly automated robotic agents.

IV. TACTILE PERCEPTION EXPERIMENTS

In this section, the effectiveness of UniT is demonstrated on a USB plug 3D pose estimation task and benchmark UniT with training a ResNet [18] from scratch, as well as other representation learning frameworks: BYOL [19], MAE [20], and the state-of-the-art tactile representation framework, T3 [21].

The task involves estimating the 3D pose of a USB plug based on its tactile image. As illustrated in Fig. 1 and our supplementary video, changes in the 3D pose of the USB plug result in altered contact configurations and corresponding variations in the tactile image. This type of 3D pose estimation is crucial for robotic insertion tasks that require high precision. This task is challenging because minor differences in the tactile images can correspond to significantly different 3D poses. The pose estimation model must accurately map these subtle tactile features to the correct 3D pose.

| | BYOL | MAE-ViT-Tiny | | | MAE-ViT-Base | | | UniT w/o VQ | | UniT | |
|------------|------|--------------|-------|-------|--------------|-------|-------|--------------------------|----------------|--------------------------|----------------|
| | | Mask Ratio | | | Mask Ratio | | | Representation Dimension | | Representation Dimension | |
| | | 0.25 | 0.5 | 0.75 | 0.25 | 0.5 | 0.75 | 8×10 | 16×20 | 8×10 | 16×20 |
| Allen Key | 1.33 | 0.337 | 0.358 | 0.374 | 0.247 | 0.273 | 0.370 | 0.225 | 0.189 | 0.156 | 0.128 |
| Small Ball | 1.06 | 0.435 | 0.685 | 0.789 | 0.526 | 0.560 | 0.388 | 0.283 | 0.185 | 0.274 | 0.166 |

TABLE I: USB plug 3D pose estimation results. Mean absolute error (in radians) on the test set of implementing representations learned from BYOL [19], MAE [18], and UniT. We test the representations trained on the Allen key dataset and the small ball dataset, respectively, as indicated in the top-right corner of Fig. 3. After the representation training phase, we freeze the encoders for all methods we benchmark here and train only the decoders on the 3D pose estimation dataset. The MAE with ViT-Base backbone has a model size of 143.20 M, whereas UniT with a representation dimension of 16×20 has a model size of 79.81 M.

| ResNet34 w/o pretrain | ResNet34 with pretrain | T3 Tiny | T3 Small | T3 Medium | T3 Large | UniT SmallBall | UniT AllenKey |
|-----------------------|------------------------|---------|----------|-----------|----------|----------------|---------------|
| 0.433 | 0.293 | 1.55 | 0.679 | 0.279 | 0.332 | 0.166 | 0.128 |

TABLE II: USB plug 3D pose estimation results. Mean absolute error (in radians) on the test set of implementing ResNet [18], T3 [21], and UniT. For T3, we utilize the pretrained model released by the authors of [21], freezing the encoder in a manner similar to our approach with other representation learning methods. In the ResNet experiments, we train both the encoder and the decoders during training on 3D pose data.

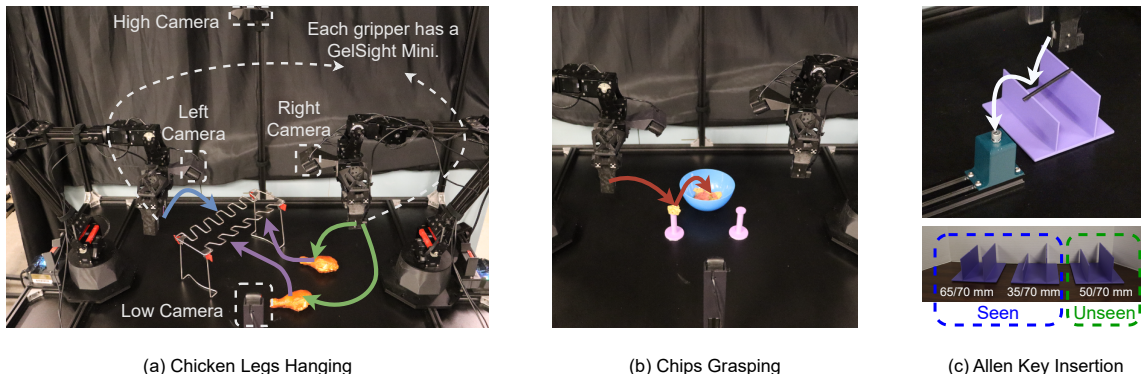


Fig. 7: Overview of three tasks and hardware setup.

| | Chicken Legs Hanging | | Chips Grasping | Allen Key Insertion | | | |
|-----------------------------|----------------------|-------------------|----------------|---------------------|-------------|-------------|--------------|
| | One Leg Inserted | Two Legs Inserted | | 65/70 mm | 35/70 mm | 50/70 mm | Total |
| Vision-Only | 9/15 | 6/15 | 8/15 | 8/10 | 3/10 | 4/10 | 15/30 |
| Visual-Tactile from Scratch | 8/15 | 5/15 | 14/15 | 6/10 | 5/10 | 6/10 | 17/30 |
| Visual-Tactile with UniT | 13/15 | 9/15 | 14/15 | 8/10 | 7/10 | 8/10 | 23/30 |

TABLE III: Success rates of policy rollout on three different tasks. We use diffusion policy [2] as the policy backbone. For UniT, we use the encoder trained on the Allen Key dataset mentioned in Section III-B for GelSight Minis on both arms and for all three tasks. In addition, we also freeze the UniT encoder when integrating it into diffusion policy, as shown in Fig. 6. In (c), the heights on the left and right sides of the rack are 65/70 mm, 35/70 mm, and 50/70 mm. These varying heights result in different in-hand poses when the Allen key is grasped. The training dataset was collected using the 65/70 mm and 35/70 mm heights.

As shown in the supplementary video, we use the OptiTrack motion capture system to label the 3D pose groundtruth. In the data collection process, human move the USB plug randomly and we record the tactile raw image as well as 3D pose groundtruth in 10 Hz.

Directly splitting the training and test sets from continuous data can cause data leakage issues. To avoid this, we have collected data in the form of episodes. An episode consists of a sequence of continuous recorded data, with no continuity overlap between different episodes. Within each episode, the movement of the USB plug by humans is random, and there is no fixed paradigm across episodes. When dividing the training and test sets, we do not use individual images as the smallest unit; instead, we use entire episodes. As a result, the data in the test set is completely absent from the training set. We use seed 42 and maintain a 9:1 training-to-test ratio to split the episodes. Ultimately, we obtained 10,111 tactile images for training and 1,229 tactile images for testing.

We use the following loss function to train the model,

which converts quaternions to angle differences $L = \mathbb{E}[2 \cdot \arccos(|\hat{q} \cdot q|)]$, where \hat{q} and q are estimated and groundtruth quaternions. For more details on this experiment, please refer to our open-source repository³.

The benchmark results are shown in Tables I and II. For representation learning methods, we freeze the encoders of UniT, MAE, BYOL, and T3 when implementing them to this 3D perception task. This approach allows us to evaluate whether the representation learning methods can truly learn generalizable and transferable tactile representations. The capability for zero-shot transfer is important when applying tactile representations across various perception and policy learning tasks with different objects (see Section V), as fine-tuning for each task and each object can be prohibitively costly.

Our experimental results clearly show that UniT delivered the best performance on this 3D pose estimation task. Moreover, compared to training from scratch, representa-

³<https://github.com/ZhengTongXu/UniT>

tion learning methods generally improve the performance of tactile perception. Finally, the experimental results also demonstrate that VQ regularization enhances the performance of downstream tasks. This indicates that a more compact tactile representation is beneficial for learning downstream tasks.

V. POLICY LEARNING EXPERIMENTS

In this section, the effectiveness of UniT in imitation learning is demonstrated. We use Aloha [3] as our hardware platform. The hardware setup is shown in Fig. 7(a). We integrate UniT into diffusion policy [2], and benchmark with vision-only diffusion policy and visual-tactile diffusion policy with tactile encoders trained from scratch. For training details, please refer to our open-source repository. We completed three tasks, as shown in Fig. 7. More details of each task are as follows.

Chicken Legs Hanging: The chicken legs hanging task is a dual-arm manipulation task in which one robotic arm grasps the rack to prevent it from moving due to the pushing force exerted while hanging chicken legs. The other arm picks up two artificial chicken legs from a table and hangs them on the rack. The precision required for this task is very high, because the width of the chicken legs and the opening of the slots on the rack are almost a perfect match. This precise alignment ensures that the chicken legs remain securely in place on the rack after being released. Moreover, this task involves rich force interactions with the objects being manipulated: the left arm applies force on the rack and stabilizes it, while the right arm exerts pressure to insert the chicken leg into the slot on the rack. In this situation, real-time tactile feedback is crucial for fully perceiving these interactions.

Chips Grasping: The Chips grasping task is also a dual-arm manipulation task. During this task, depending on whether the chips are on the left or right support stand, the corresponding robot arm picks up the chips and places them into a bowl. To accommodate the maximum width of the grippers, we resized the chips from their original dimensions. The challenge of this task lies in the fragility of the chips, which necessitates precise control over the gripper width. The gripper must adjust accurately to accommodate the shape and size of the chips. Inadequate adjustment may lead to either missing the grasp or crushing the chips. In this situation, real-time tactile feedback is crucial because relying solely on visual feedback makes it difficult to accurately determine the state of the grasp. This can easily lead to missing the grasp or breaking the chips when handling different sizes of chips.

Allen Key Insertion: The Allen key insertion task requires the robot to grasp a Allen Key on a rack and then insert the Allen Key into a nut. We used a 6 mm nut and an Allen key with 5.5 mm head. In this configuration, the Allen key can still be used to tighten and loosen the nut effectively after insertion. Therefore, the precision requirement for this insertion is at the millimeter level. Given that Aloha is a low-cost robot, its repeatability in terms of precision is not high, which adds significant challenges to this task.

During data collection and policy rollout, we modify the size of the rack (the height difference between the supports on each side), which in turn affects the angle of the Allen key when it is grasped in-hand by the robot. We collected data for two different types of racks in the training set. During policy rollout, we tested three different types of rack, including a rack that was completely unseen in the training set, representing out-of-distribution data (see Fig. 7(c)).

The tactile modality serves two pivotal functions in this task: 1) Given the variety of racks, leveraging tactile modality to gather information on the Allen key’s in-hand pose is vital for appropriately adjusting the pose of the end effector during insertion. 2) Insertion often proves challenging when aligning the Allen key with the nut on the first attempt, often leading to minor misalignments. In these instances, tactile feedback plays a critical role in interactively refining the policy to accurately guide the Allen key into the nut.

The results of the policy rollout on these three tasks are shown in Table III. It is evident that the visual-tactile policy with UniT delivers the best performance on each task. As described earlier, the three tasks presented here involve rich robot-object-environment interactions. Our experimental results highlight two important points regarding these types of tasks: 1) The tactile modality is crucial for manipulation tasks with rich interactions, where relying solely on vision often fails to deliver optimal performance. 2) Compared to treating tactile images as regular visual images and training encoders from scratch, using UniT significantly enhances the effectiveness of integrating the tactile modality into the policy.

For more detailed information about our experimental results, see the supplementary video and the project website⁴.

VI. DISCUSSION AND FUTURE WORK

Due to the unique nature of tactile images, traditional visual representation learning methods may not be entirely suitable for tactile images. For example, in MAE, much of the masked input is ineffective tactile background because the useful information in a tactile image is primarily located where the object contacts the sensor pad. Inspired by the compact color distribution of tactile images, we utilized VQVAE to learn a compact latent space. This approach has been shown to be effective for representation learning specifically tailored to tactile images. Finally, two promising research directions are proposed:

1. **Extension to Soft Objects:** Our current framework has been validated only on rigid objects. However, the tactile features of soft objects pose a new set of challenges due to their complexity [11]. Exploring how to learn a unified tactile representation that works effectively for both rigid and soft objects should be a promising topic.

2. **Physics-Informed Tactile Representations:** Soft objects often correlate with complex physical properties, such as stiffness [11]. In addition, other studies have highlighted

⁴<https://zhengtongxu.github.io/unifiedtactile.github.io/>

the potential of tactile sensing in understanding the physical world [12], [13]. Researching how to develop physics-informed representations that can integrate with diverse tasks (such as estimation of physical properties, physics-inspired robot manipulation, and AI4Science) could be highly intriguing.

VII. ACKNOWLEDGEMENTS

This work was partially supported by the United States Department of Agriculture (USDA; No. 2023-67021-39072 and No. 2024-67021-42878). This article solely reflects the opinions and conclusions of its authors and not of USDA.

REFERENCES

- [1] C. Chi, Z. Xu, C. Pan, E. Cousineau, B. Burchfiel, S. Feng, R. Tedrake, and S. Song, "Universal manipulation interface: In-the-wild robot teaching without in-the-wild robots," *arXiv preprint arXiv:2402.10329*, 2024.
- [2] C. Chi, S. Feng, Y. Du, Z. Xu, E. Cousineau, B. Burchfiel, and S. Song, "Diffusion policy: Visuomotor policy learning via action diffusion," in *Proceedings of Robotics: Science and Systems (RSS)*, 2023.
- [3] T. Z. Zhao, V. Kumar, S. Levine, and C. Finn, "Learning fine-grained bimanual manipulation with low-cost hardware," *arXiv preprint arXiv:2304.13705*, 2023.
- [4] C. Wang, H. Shi, W. Wang, R. Zhang, L. Fei-Fei, and C. K. Liu, "Dexcap: Scalable and portable mocap data collection system for dexterous manipulation," *arXiv preprint arXiv:2403.07788*, 2024.
- [5] Y. Ze, G. Zhang, K. Zhang, C. Hu, M. Wang, and H. Xu, "3d diffusion policy," *arXiv preprint arXiv:2403.03954*, 2024.
- [6] W. Yuan, S. Dong, and E. H. Adelson, "GelSight: High-resolution robot tactile sensors for estimating geometry and force," *Sensors*, vol. 17, no. 12, p. 2762, 2017.
- [7] S. Wang, Y. She, B. Romero, and E. Adelson, "GelSight Wedge: Measuring high-resolution 3D contact geometry with a compact robot finger," in *Proc. IEEE Int. Conf. Robot. Autom.*, 2021, pp. 6468–6475.
- [8] Y. She, S. Wang, S. Dong, N. Sunil, A. Rodriguez, and E. Adelson, "Cable manipulation with a tactile-reactive gripper," *Int. J. Robot. Res.*, vol. 40, no. 12-14, pp. 1385–1401, 2021.
- [9] M. Bauza, A. Bronars, and A. Rodriguez, "Tac2pose: Tactile object pose estimation from the first touch," *The International Journal of Robotics Research*, vol. 42, no. 13, pp. 1185–1209, 2023.
- [10] D. Ma, E. Donlon, S. Dong, and A. Rodriguez, "Dense tactile force estimation using gelslim and inverse fem," in *Proc. IEEE Int. Conf. Robot. Autom.*, 2019, pp. 5418–5424.
- [11] Z. Xu and Y. She, "Letac-mpc: Learning model predictive control for tactile-reactive grasping," *arXiv preprint arXiv:2403.04934*, 2024.
- [12] H.-J. Huang, X. Guo, and W. Yuan, "Understanding dynamic tactile sensing for liquid property estimation," *arXiv preprint arXiv:2205.08771*, 2022.
- [13] X. Guo, H.-J. Huang, and W. Yuan, "Estimating properties of solid particles inside container using touch sensing," in *2023 IEEE/RSJ International Conference on Intelligent Robots and Systems (IROS)*. IEEE, 2023, pp. 8985–8992.
- [14] L. Wang, J. Zhao, Y. Du, E. H. Adelson, and R. Tedrake, "Poco: Policy composition from and for heterogeneous robot learning," *arXiv preprint arXiv:2402.02511*, 2024.
- [15] Y. Gu and Y. Demiris, "Vttb: A visuo-tactile learning approach for robot-assisted bed bathing," *IEEE Robotics and Automation Letters*, 2024.
- [16] K. Yu, Y. Han, M. Zhu, and Y. Zhao, "Mimictouch: Learning human's control strategy with multi-modal tactile feedback," *arXiv preprint arXiv:2310.16917*, 2023.
- [17] S. Athar, G. Patel, Z. Xu, Q. Qiu, and Y. She, "Vistac towards a unified multi-modal sensing finger for robotic manipulation," *IEEE Sensors Journal*, 2023.
- [18] K. He, X. Zhang, S. Ren, and J. Sun, "Deep residual learning for image recognition," in *Proc. IEEE Conf. Comput. Vis. Pattern Recognit.*, 2016, pp. 770–778.
- [19] J.-B. Grill, F. Strub, F. Altché, C. Tallec, P. Richemond, E. Buchatskaya, C. Doersch, B. Avila Pires, Z. Guo, M. Gheshlaghi Azar *et al.*, "Bootstrap your own latent: a new approach to self-supervised learning," *Advances in neural information processing systems*, vol. 33, pp. 21 271–21 284, 2020.
- [20] K. He, X. Chen, S. Xie, Y. Li, P. Dollár, and R. Girshick, "Masked autoencoders are scalable vision learners," in *Proceedings of the IEEE/CVF conference on computer vision and pattern recognition*, 2022, pp. 16 000–16 009.
- [21] J. Zhao, Y. Ma, L. Wang, and E. H. Adelson, "Transferable tactile transformers for representation learning across diverse sensors and tasks," 2024.
- [22] I. Guzey, Y. Dai, B. Evans, S. Chintala, and L. Pinto, "See to touch: Learning tactile dexterity through visual incentives," *arXiv preprint arXiv:2309.12300*, 2023.
- [23] T. Lin, Y. Zhang, Q. Li, H. Qi, B. Yi, S. Levine, and J. Malik, "Learning visuotactile skills with two multifingered hands," *arXiv:2404.16823*, 2024.
- [24] W. Yang, A. Anglraud, R. S. Pieters, J. Pajarinen, and J.-K. Kämäräinen, "Seq2seq imitation learning for tactile feedback-based manipulation," in *2023 IEEE International Conference on Robotics and Automation (ICRA)*. IEEE, 2023, pp. 5829–5836.
- [25] Z. Liu, C. Chi, E. Cousineau, N. Kuppuswamy, B. Burchfiel, and S. Song, "Maniwav: Learning robot manipulation from in-the-wild audio-visual data," *arXiv preprint arXiv:2406.19464*, 2024.
- [26] X. Li, V. Belagali, J. Shang, and M. S. Ryo, "Crossway diffusion: Improving diffusion-based visuomotor policy via self-supervised learning," *arXiv preprint arXiv:2307.01849*, 2023.
- [27] J. Pari, N. M. Shafiqullah, S. P. Arunachalam, and L. Pinto, "The surprising effectiveness of representation learning for visual imitation," *arXiv preprint arXiv:2112.01511*, 2021.
- [28] G. Cao, J. Jiang, D. Bollegala, and S. Luo, "Learn from incomplete tactile data: Tactile representation learning with masked autoencoders," in *2023 IEEE/RSJ International Conference on Intelligent Robots and Systems (IROS)*. IEEE, 2023, pp. 10 800–10 805.
- [29] C. Sferrazza, Y. Seo, H. Liu, Y. Lee, and P. Abbeel, "The power of the senses: Generalizable manipulation from vision and touch through masked multimodal learning," 2023.
- [30] M. Polic, I. Krajacic, N. Lepora, and M. Orsag, "Convolutional autoencoder for feature extraction in tactile sensing," *IEEE Robotics and Automation Letters*, vol. 4, no. 4, pp. 3671–3678, 2019.
- [31] F. Yang, C. Feng, Z. Chen, H. Park, D. Wang, Y. Dou, Z. Zeng, X. Chen, R. Gangopadhyay, A. Owens, and A. Wong, "Binding touch to everything: Learning unified multimodal tactile representations," *arXiv:2401.18084*, 2024.
- [32] P. Esser, R. Rombach, and B. Ommer, "Taming transformers for high-resolution image synthesis," in *Proceedings of the IEEE/CVF conference on computer vision and pattern recognition*, 2021, pp. 12 873–12 883.
- [33] A. Van Den Oord, O. Vinyals *et al.*, "Neural discrete representation learning," *Advances in neural information processing systems*, vol. 30, 2017.
- [34] R. Rombach, A. Blattmann, D. Lorenz, P. Esser, and B. Ommer, "High-resolution image synthesis with latent diffusion models," in *Proceedings of the IEEE/CVF conference on computer vision and pattern recognition*, 2022, pp. 10 684–10 695.
- [35] Z. Fei, M. Fan, L. Zhu, J. Huang, X. Wei, and X. Wei, "Masked auto-encoders meet generative adversarial networks and beyond," in *Proceedings of the IEEE/CVF Conference on Computer Vision and Pattern Recognition*, 2023, pp. 24 449–24 459.
- [36] J. Donahue and K. Simonyan, "Large scale adversarial representation learning," *Advances in neural information processing systems*, vol. 32, 2019.
- [37] Y. Wu and K. He, "Group normalization," in *Proceedings of the European conference on computer vision (ECCV)*, 2018, pp. 3–19.
- [38] J. Hu, L. Shen, and G. Sun, "Squeeze-and-excitation networks," in *Proceedings of the IEEE conference on computer vision and pattern recognition*, 2018, pp. 7132–7141.